F. Wang
Department of Mechanical Engineering,
University of New Brunswick,
Fredericton, N.B. Canada;
Presently University of Waterloo,
Waterloo, Canada

Y. Hwu
R & D Department,
China Steel Corporation, Taiwan

J. G. Lenard
Department of Mechanical Engineering,
University of New Brunswick,
Fredericton, N.B. Canada E3B 5A3

Simulation of the Variation of Strain Rates During a Rolling Pass in Compression Tests

A Nb-V steel's response to constant true strain rate compression was compared to its behavior when the strain rate varied as during a rolling pass. The constitutive behavior during the two types of tests was found not to differ in a significant manner.

Introduction

The traditional way of determining the constitutive behavior of metals is to conduct a set of experiments in tension, compression or torsion, at preselected temperatures and constant true strain rates and use the resulting data in calculations of the process parameters. The manner in which the constitutive data is employed is far from settled. Empirical relations may be established and there are several from which to choose or multidimensional data-banks may be set up with strain, rate of strain, temperature, prior thermal-mechanical history and pre-test grain sizes as the independent variables from which the results are retrieved as required (Lenard et al., 1987).

In order to reduce the number of variables during testing for strength, the strain rate is usually kept constant. It is recognized, however, that in metal-forming operations the rate of straining does not remain constant and it was this fact that gave rise to the present project.

McQueen and Jonas (1971) refer to the variation of strain rate during extrusion and state that

> . . . "The ideal way to determine power and the maximum flow stress is to use a test programmed to simulate the strain rate profile of the working process."

Results, obtained by the plane-strain compression test, which was developed by Watts and Ford (1952), were discussed by Weinstein and Matsufuji (1968). They concluded that better correspondence of predicted and measured roll forces and torques was obtained by the use of plane strain material strength data than by the use of uniaxial compression data.

Kokado et al. (1985) refer to the variation of the rate of strain from entry to exit during strip rolling. Wray (1986), in order to model the hot flow strength of a niobium bearing microalloyed steel, uses the strain rate as a variable in the roll gap.

Sah and Sellars (1979) studied the dependence of the softening processes in hot, plane strain compression of a ferritic stainless steel. They subjected the samples to continuously increasing or continuously decreasing strain rates and compared the response to that exhibited using the traditional constant true strain rate mode. In a single deformation experiment, the constant strain rate was taken to equal 5.5 s^{-1}, the increasing strain rate - to simulate extrusion - varied from zero to about 18 s^{-1}, in an exponential fashion - while in the test, simulating flat rolling, the strain rate dropped from about 6.5 s^{-1} to zero. The steel's response appeared to be strongly dependent on the strain rate history.

In a recent series of publications Urcola and Sellars (1987a, 1987b, and 1987c) studied the constitutive behavior of a ferritic stainless steel and two types of aluminum when subjected to plane strain compression under conditions of varying strain rates. They found that when the rates of strain were increased or decreased by at least one-half order of magnitude, the metal's resistance to deformation also changed significantly. Further, they concluded that the stainless steel and the Al – 1 percent Mg follow a mechanical equation of state but that commercially pure aluminum does not.

To the best of the authors' knowledge, no results from compression tests, in which the rate of strain varies exactly as in flat rolling, have been published. This then led to the formulation of the present project whose purpose is stated as a study to discover whether that variation of strain rate, when simulated in compression testing, would effect the shape or the magnitude of the flow curves.

Rate of Strain During Flat Rolling

Assuming that the rolls remain cylindrical during the pass and sticking friction exists between the strip and the work rolls, it is simple to show that in the roll gap the strain rate varies from a maximum at entry to zero at exit, as given below:

$$\dot{\epsilon}^{(1)} = \frac{2R' \sin\phi \dot{\phi}}{h_2 + 2R'(1 - \cos\phi)} \tag{1}$$

Contributed by the Materials Division for publication in the JOURNAL OF ENGINEERING MATERIALS AND TECHNOLOGY. Manuscript received by the Materials Division February 2, 1988; revised manuscript received April 7, 1989.

Downloaded From: https://materialstechnology.asmedigitalcollection.asme.org on 06/29/2019 Terms of Use: http://www.asme.org/about-asme/terms-of-use
Copyright © 1989 by ASME

The mean strain rate is then obtained by integrating over the theoretical contact length and becomes

$$\dot{\epsilon}_m^{(1)} = \frac{\dot{\phi}}{\phi_1} \ln \frac{h_1}{h_2} \tag{2}$$

While the assumption of the existence of sticking friction, at least for hot rolling, has been recommended by researchers (Alexander, 1972) several studies have shown that it does not represent actual conditions very well (Sparling, 1977; Lenard, 1986). If slipping between the rolls and the strip is accounted for the variation of the strain rate from entry to exit will be affected significantly. Roberts' (1983) formula may then be used for it gives the strain rate experienced by the strip in terms of the strip height at the neutral point (h_α) and its location (α) as

$$\dot{\epsilon}^{(2)} = 2v_r h_\alpha \cos\alpha \tan\phi / h^2 \tag{3}$$

where v_r is the surface velocity of the roll. The average strain rate is also derived by Roberts; it is

$$\dot{\epsilon}_m^{(2)} = \frac{v_r h_\alpha \cos\alpha}{h_1 h_2} \sqrt{(h_1 - h_2)/R'} \tag{4}$$

where the usual "small angle" approximations have been made e.g., $\tan\phi \cong \phi$ and $\phi^2 \cong 2(1-\cos\phi)$. In order to use equations (3) and (4) for calculations one must, of course, know the location of the neutral point. One of the usual approaches is to follow Roberts and let $\alpha = \phi_1/2$ which leads to

$$h_\alpha = (3h_2 + h_1)/4 \tag{5}$$

and the mean strain rate then becomes

$$\dot{\epsilon}_m^{(2)} = \frac{v_r (3h_2 + h_1)\cos\alpha}{4h_1 h_2} \sqrt{(h_1 - h_2)/R'}. \tag{6}$$

Perhaps a more natural approach is to take the forward slip of the rolled product into account which is defined as

$$f = (v_2 - v_r)/v_r \tag{7}$$

where v_2 is the exit velocity of the strip and hence, measureable with relative ease. Then, letting $\dot{\phi}$ in equation (1) represent the angular velocity of a point on the strip surface, the strain rate as a function of the angular variable becomes

$$\dot{\epsilon} = 2v_r h_2 (1+f)\tan\phi / h^2 \tag{8}$$

whose average value in the pass is obtained as

$$\dot{\epsilon}_m = \frac{2v_r h_2 (1+f)}{\phi_1 (h_2 + 2R')} \left[\frac{1}{h_2} - \frac{1}{h_1} + \frac{1}{(h + 2R')} \ln \left(\frac{h_1}{h_2} \frac{2R'}{h_2 - h_1 + 2R'} \right) \right]. \tag{9}$$

The similarity between the strain rates given by equations (3) and (8) is immediately apparent. The nature of the variation of $\dot{\epsilon}$ is pedicted to be identical by both. The magnitudes differ significantly however, and it is the ratio of the constant terms in (3) and (8) that governs those magnitudes.

It is, of course, the different definitions of the neutral angle that cause the discrepancies. In equation (3) the assumption that the neutral plane is halfway between the entry and exit was made. For equation (8) considerations of the equilibrium of the strip in the roll gap yielded the required information.

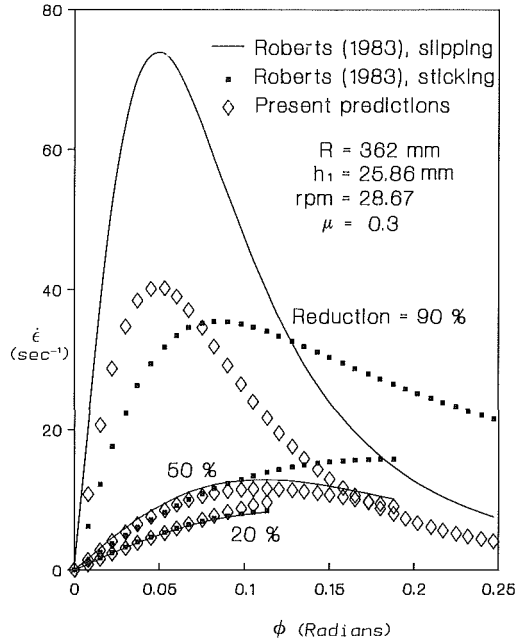

Fig. 1 Comparison of the variation of strain rates as predicted by Roberts and the present authors

The second consideration is felt to be the more realistic one and predictions from equation (8) are believed to be close to reality.

A comparison of the variation of the strain rate in the roll gap as predicted by the above formulas requires an expression for the forward slip in terms of the process parameters. A useful equation, based on Ekelund's relation for the location of the neutral angle is given by Cao (1979), giving the forward slip as a function of the reduction, roll radius and the coefficient of friction in the form

$$f = \frac{h_1 - h_2}{4h_2} \left(1 - \frac{1}{2\mu} \sqrt{\frac{h_1 - h_2}{R'}} \right)^2 \tag{10}$$

which was obtained with the usual small angle assumption.

For a typical set of parameters Fig. 1 presents each of the three rates of strain, as given by equations (1), (3), and (8). Significant differences in strain rate predictions are observed, especially when slipping is accounted for in the derivations and large reductions are considered. At lower strains all three formulas indicate that $\dot{\epsilon}$ decreases from entry to exit. In excess of $r = 30$ percent, the rates of strain, given by equations (3) and (8) increase to a maximum value before they fall to zero on exit.

Experimental Equipment, Material, and Procedure

Equipment. The experiments were carried out on a microprocessor controlled servohydraulic testing system, built around an Instron Model 1331/1332 unit.

Details of a subroutine in the control program driving the servovalve determine the motion of the piston. By prescribing

Nomenclature

R' = flattened roll radius
V = voltage
f = forward slip
h = strip thickness
h_1, h_2 = strip thickness at entry and exit, respectively
h_α = strip thickness at the neutral plane
r = reduction
v_r = roll surface velocity
v_2 = exit velocity
α = location of the neutral plane
ϵ_{ss} = steady state strain
ϵ = strain rate
$\dot{\epsilon}_m$, $\dot{\epsilon}$ = mean strain rate
μ = coefficient of friction
ϕ = angular variable
ϕ_1 = roll gap angle
$\dot{\phi}$ = angular velocity of the rolls
ω = angular velocity of the strip

Downloaded From: https://materialstechnology.asmedigitalcollection.asme.org on 06/29/2019 Terms of Use: http://www.asme.org/about-asme/terms-of-use

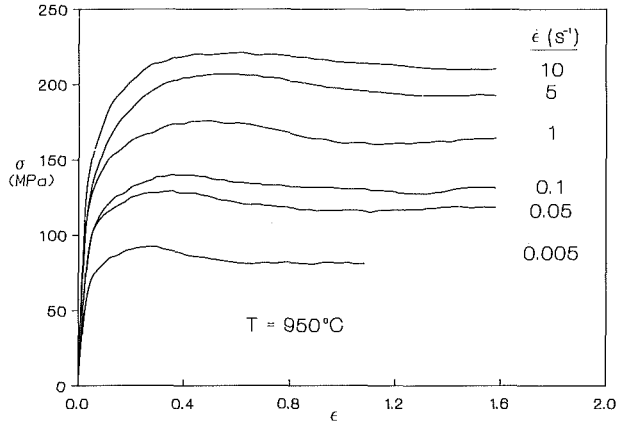

Fig. 2 Constant strain rate flow curves at 950°C

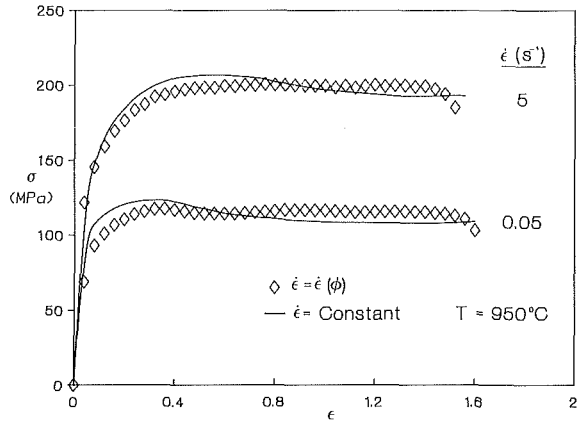

Fig. 3 Flow curves resulting from constant and varying strain rate experiments

an exponentially decaying voltage the actuator travels to cause constant true strain rate throughout its stroke.

Alternatively, by transforming the independent variable in equation (8) from angle to time, integrating to solve for the current height and using the result to drive the servovalve defines its response such that the strain rate, during compression of the samples, varies as in flat rolling.

The time-voltage signal to be sent to the servovalve is developed next. This requires an expression of the angular velocity of the strip, given by

$$\omega(\phi) = v_2 h_2/(R' h\cos\phi). \tag{11}$$

The incremental change in the angular variable is $\Delta\phi = \omega(\phi)\,\Delta t$ where Δt is the time increment. The roll gap angle is increased accordingly and the current strip height is then obtained from

$$h(t) = h_2 + 2R'[1 - \cos\phi(t)] \tag{12}$$

and the voltage, to be generated by the processor is defined as

$$V(t) = 1 - [h(t)/h_2]^{\sqrt{3}/2} \tag{13}$$

and passed to the servovalve.

Strain rates of up to 15 s^{-1} on the 1332 frame and up to 50 s^{-1} on the 1331 are reached, using specimens not higher than 20 mm. The dynamic response of the system is adequate; even at high speeds, when the time taken to overcome the inertia of the servovalve is significant, command and feedback signals differ by no more than 10 percent. Data acquisition is achieved by the A/D converter of the computer and the resulting true stress - true strain curves are obtained directly on the attached plotter. Further, to simulate the conditions in the finishing train of a hot strip mill, interrupted compression testing, up to 20 stages, can be conducted, within a highly stable, split resistance furnace. Details of the testing facility have been published by Lenard (1985).

Material The material was obtained in the form of hot rolled strip. Its chemical composition in weight percent is given below:

C	Mn	V	Nb	P	Al	S	Cr	Ni	Si	Cu	Fe
.13	1.55	.049	.028	.013	.07	.008	.23	.33	.28	.34	rest

The nitrogen content was 50 ppm for the steel.

Procedure. The pretest heat-treatment involved annealing the 6 mm diameter, 9 mm long axially symmetrical specimens for 2 hours at 1000°C followed by cooling in air and solution treatment at 1250°C for 20 minutes. Quenching in water ensured that all alloys remained in solution.

The samples, whose ends were recessed to a depth of 0.1 mm, were placed in the preheated furnace and after a wait of 5 minutes the compression test was performed. Molten glass lubricant was used to minimize friction at the ram-sample interface.

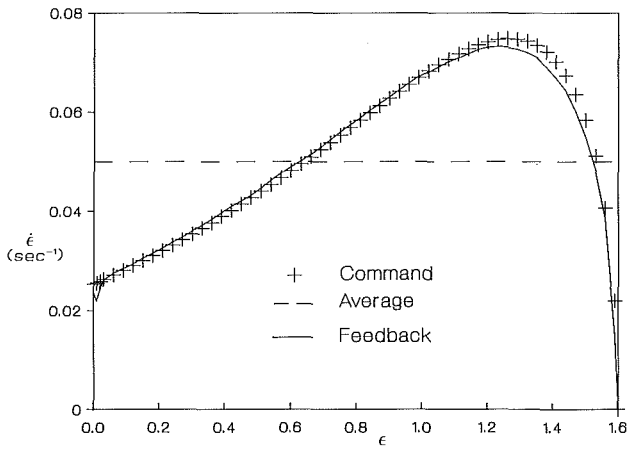

Fig. 4 Dynamic response of the testing system; $\dot{\epsilon} = 0.05\ s^{-1}$

Results and Discussion

As the first step in evaluating the steel's response to variations in the rate of straining during upsetting, its constant strain rate behavior was established. The flow curves, obtained in uniaxial compression at 950°C are shown in Fig. 2 for strain rates of 0.005, 0.05, 0.1, 1, 5, and 10 s^{-1}. The curves were corrected for frictional effects, using friction factors that were determined from hot ring tests (Wang, 1988). The constitutive behavior usual for microalloyed steels is observed; the initial hardening is followed by softening due to dynamic recrystallization. Steady-state flow occurs beyond strains of approximately 0.7 for the slower tests and about unity for the higher rates.

Experiments, during which the rates of strain vary were conducted next.

Two tests were performed to simulate a reduction of 75 percent, both at 950°C and at average rates of strain of 5 s^{-1} and 0.05 s^{-1} respectively. The corresponding flow curves are shown in Fig. 3. In both variations of $\dot{\epsilon}$ as prescribed by equation (8) were used, making certain that the average values equal those of the constant rate tests. In the figure the solid lines represent behavior under constant strain rate conditions and the symbols denote the varying strain rate response.

Downloaded From: https://materialstechnology.asmedigitalcollection.asme.org on 06/29/2019 Terms of Use: http://www.asme.org/about-asme/terms-of-use

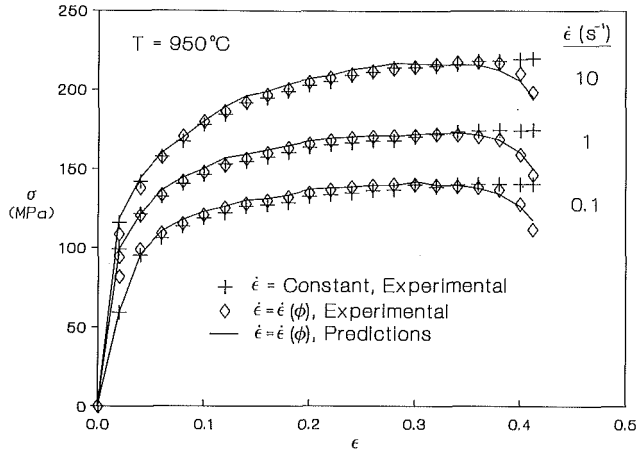

Fig. 5 Flow curves for 30 percent reduction

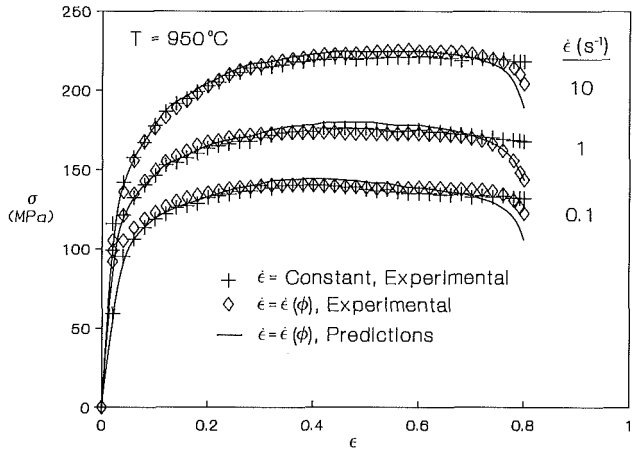

Fig. 6 Flow curves for 50 percent reduction

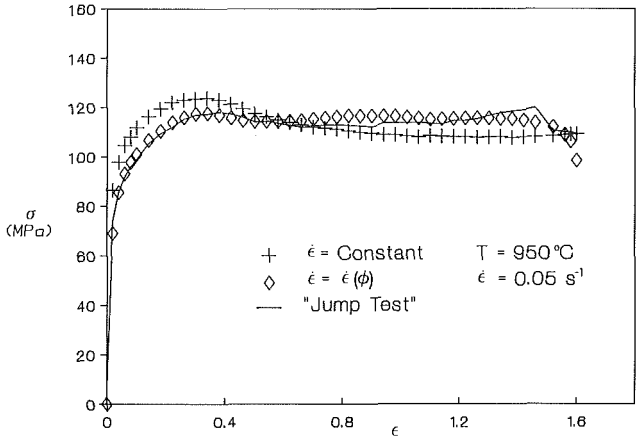

Fig. 7 Flow curves of a 9 stage "jump" test, a constant and a varying strain rate experiment

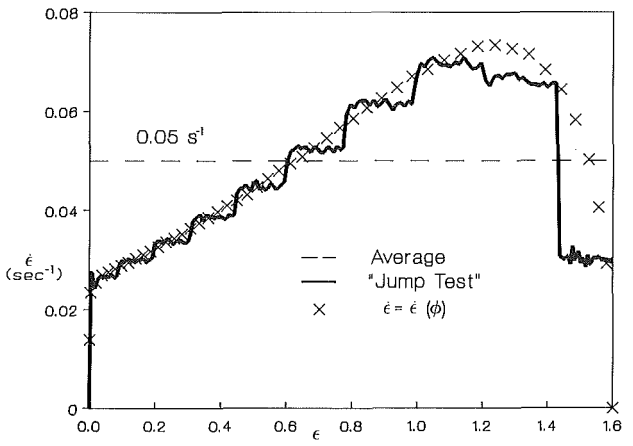

Fig. 8 Dynamic response of the testing system during the jump test

In analyzing the response of the metal it is helpful to consider the dynamic response of the testing system during the experiments. These are shown in Fig. 4 for the 0.05 s^{-1} flow curve depicting the "command" signal, which refers to the strain rate variation given by equation (8) in addition to the "feedback," giving the actual strain rates, experienced by the sample. It is observed that the testing system is performing adequately.

The varying strain rate test loads the sample at a significantly slower rate at the beginning than in the constant strain rate test. In both experiments of Fig. 3 this results in the constant strain rate flow curves indicating higher strength sooner than the varying strain rate curves.

At $\dot{\epsilon} = 0.05\ s^{-1}$ the varying and constant rate curves reach plateaux of 115 and 120 MPa magnitudes, respectively. The strains at which the peak strengths occur are identical for the two tests at $\epsilon_p = 0.34$. The strain rate experienced by the sample of the varying rate is 0.04 s^{-1} at that level of strain, indicating that the steel's strength has not "caught up" yet with the rate. Its metallurgical structure requires some more time to reach the constant strain rate expectations.

The higher rate experiment shows essentially similar behavior for both constant and varying $\dot{\epsilon}$. Some differences of strength are observed, especially near the peak strain.

It is interesting to compare the current results to those shown in Fig. 1 of Sah and Sellars (1979). Some similarities in behavior may be observed, especially the delayed reaction of the steel's resistance to deformation. In these authors' varying strain rate test the initial value of $\dot{\epsilon}$ equals 6.5 s^{-1}, 1 s^{-1} more than the constant rate experiment. This causes the flow curve corresponding to the former rate to be about 4 percent above that of the latter at the start. As the strain rate decreases the strength also falls. At a strain of 0.42 the varying rate dips below 5.5 s^{-1} but the corresponding crossover of the stress-strain curves happens only at $\epsilon = 0.53$, indicating the time required for the microstructural evolution.

Equation (8) indicates that the strain rate variation during the compression test is a function of the total reduction as well. The next set of experiments were designed to examine the effect of this dependence on the metal's response. The results are shown in Figs. 5 and 6, both of them giving flow curves for corresponding sets of constant and varying strain rate tests.

For a reduction of 30 percent - see Fig. 5 - and for 50 percent - see Fig. 6 - the earlier conclusions are reinforced. While some local changes in the metal's resistance to deformation are evident, no significant variations are found.

The results presented in Figs. 3, 5, and 6 were somewhat unexpected and a little bit surprising. As the rate of strain increased to a value about 40 percent in excess of the average, the material's strength was expected to rise, reflecting its increased resistance to deformation. This however did not occur in any of the experiments and the stress levels required for steady state deformation in the constant true strain rate tests are found to be practically identical to the corresponding magnitudes in the varying strain rate tests.

In order to obtain convincing proof of the lack of significant strength variation, the experiment using $\dot{\epsilon} = 0.05\ s^{-1}$ was repeated. However, instead of allowing the voltage of equa-

Downloaded From: https://materialstechnology.asmedigitalcollection.asme.org on 06/29/2019 Terms of Use: http://www.asme.org/about-asme/terms-of-use

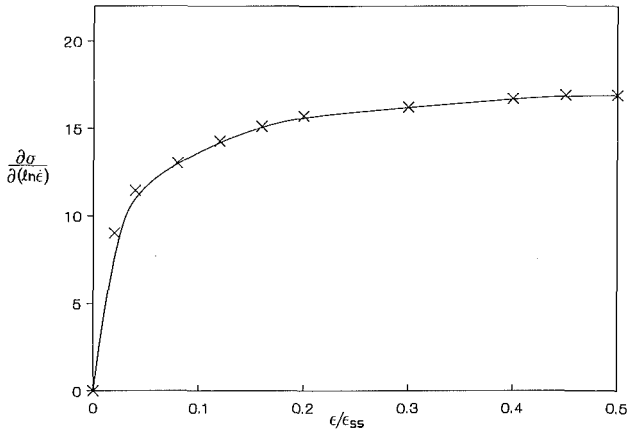

Fig. 9 $\partial\sigma/\partial(\ln\dot{\epsilon})$ versus ϵ/ϵ_{ss}

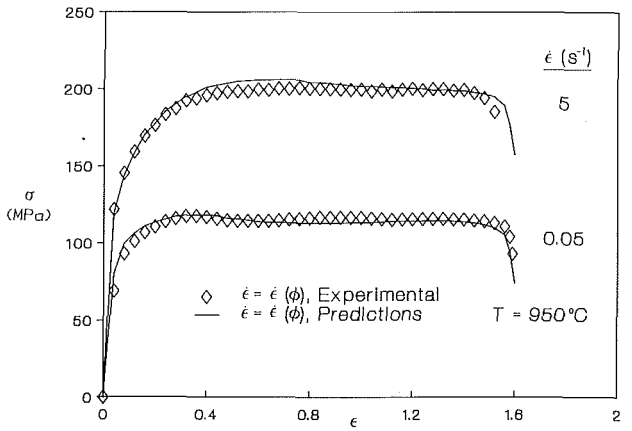

Fig. 10 Flow curves predicted by a mechanical equation of state

tion (8) to drive the servovalve, a 9-stage "jump test" was conducted such that the strain rate during each "jump" remained constant. The resulting flow curve is compared to its constant and varying $\dot{\epsilon}$ counterparts in Fig. 7.

The magnitudes of the jumps in each stage were chosen such that the strain rate variation of Fig. 3 was approximated. Figure 8 shows the actual response of the testing machine as well, superimposed on the $\dot{\epsilon} - \epsilon$ curves of Fig. 4. As observed, the flow curves corresponding to the jump test and to the continuously varying $\dot{\epsilon}$ experiment are not significantly different. Both show practically identical peak strengths and peak strains. Both indicate that the rates of hardening and softening reach equilibrium beyond a strain of about 0.6. The earlier conclusion, that variations of the strain rate as given by equation (8), do not produce significant changes in constitutive behavior, is reinforced.

Urcola and Sellars (1987a) have indicated that a ferritic stainless steel's behavior follows a mechanical equation of state. Assuming that this is valid for the present material as well, a simple analysis, utilizing an equation of state, may also be used to substantiate the above results. In order to do this, it is useful to consider the Arrhenius equation

$$\dot{\epsilon} = A\,[\sinh(\alpha\sigma)]^n \exp(-Q/RT) \tag{14}$$

which for high stress levels and constant temperatures can be written as

$$\dot{\epsilon} = B\exp(\beta\sigma). \tag{15}$$

Equation (15) is inverted to give the material's strength as

$$\sigma = a\ln\dot{\epsilon} + b \tag{16}$$

where a and b depend on the magnitude of the current strain. The slope, $a = \partial\sigma/\partial(\ln\dot{\epsilon})$, may be obtained from the flow curves of Fig. 2 and for a temperature of 950°C its average values are given in terms of the ratio of strain and the steady-state strain in Fig. 9. Note that beyond the peak strain the curve is essentially flat, indicating that in that regime the slope is independent of ϵ/ϵ_{ss}. The parameter b is then determined at a particular value of the strain rate,

$$b(\epsilon/\epsilon_{ss}) = \sigma(\epsilon/\epsilon_{ss})\,|_{\bar{\dot{\epsilon}}} - \frac{\partial\sigma(\epsilon/\epsilon_{ss})}{\partial(\ln\dot{\epsilon})}(\ln\bar{\dot{\epsilon}}) \tag{17}$$

and the resistance to deformation, in a varying strain rate experiment, whose average value is $\bar{\dot{\epsilon}}$, may be written as

$$\sigma(\epsilon/\epsilon_{ss}) = (\epsilon/\epsilon_{ss})\,|_{\bar{\dot{\epsilon}}} + \frac{\partial\sigma(\epsilon/\epsilon_{ss})}{\partial(\ln\dot{\epsilon})}\ln(\dot{\epsilon}/\bar{\dot{\epsilon}}). \tag{18}$$

In the above ϵ_{ss} refers to the strain at which steady state conditions are reached.

The validity of the model is observable in Fig. 10 where the flow curves of Fig. 3 are repeated and the predictions of equation (18) are also shown. The agreement is quite apparent, indicating that for the parameters used the metal's behavior appears to follow a mechanical equation of state. It is realized that when precipitation is significant this conclusion may not remain valid.

The predictions of the model are also shown in Figs. 5 and 6 for the corresponding experiments.

Conclusions

The high temperature constitutive behavior of a Nb-V microalloyed steel was studied. Cylindrical samples were subjected to compression at constant true strain rates and the resulting flow curves were compared to those obtained when the rate of strain varied as in a rolling pass. The steel's response appeared to be essentially unchanged in the two types of tests, except at the very end of the varying rate compression where the stress required to continue the deformation decreased sharply. Decreasing flow strength indicates a decrease in dislocation density and thus a decrease in the stored energy. Therefore, the softening kinetics during an unloading period at that strain level may be affected substantially. This was also observed by Sah and Sellars (1979) during an examination of the microstructures of a ferritic stainless steel, subjected to varying and constant strain rate testing.

Acknowledgments

The authors are grateful for the financial assistance received from the Natural Sciences and Engineering Research Council of Canada and NATO, under Special Research Grant #390/83. F. Wang wishes to express his thanks to the Xi'an Jiaotong University, allowing him to study at the University of New Brunswick. Y. Hwu is grateful to the China Steel Corporation of Taiwan, permitting him to spend a year as a Visiting Scientist at the University of New Brunswick. The authors wish to thank Dr. J. J. Jonas of McGill University, Montreal, Canada for his helpful discussion. The assistance of The Algoma Steel Corporation, Ltd. is also acknowledged.

References

Alexander, J. M., 1972, "On the Theory of Rolling," *Proc. Royal Society of London*, Vol. A326, pp. 535–563.

Cao, H. (ed.), 1979, *Fundamentals of Plastic Deformation Mechanics and Principles of Rolling*, Mechanical Industry Press, Beijing, PRC (in Chinese).

Kokado, J., Hatta, N., Takuda, H., Kikuchi, S., and Hirabayashi, T., 1985, "Prediction of Mill Load in Hot Strip Mill Rolling," *Steel Research*, Vol. 56, pp. 619–624.

Lenard, J. G., 1985, "Development of an Experimental Facility for Single and Multistage, Constant Strain Rate Compression," ASME JOURNAL OF ENGINEERING MATERIALS AND TECHNOLOGY, Vol. 107, pp. 125–131.

Downloaded From: https://materialstechnology.asmedigitalcollection.asme.org on 06/29/2019 Terms of Use: http://www.asme.org/about-asme/terms-of-use

Lenard, J. G., 1986, "Experimental Substantiation of Mathematical Models of Flat Rolling," *Proc. Symp. on Computer Modelling of Fabrication Processes and Constitutive Behaviour of Metals*, Ottawa, Canada, pp. 75–102.

Lenard, J. T., Wang, F., and Nadkarni, G., 1987, "The Role of Constitutive Formlation in the Analysis of Hot Rolling," ASME JOURNAL OF ENGINEERING MATERIALS AND TECHNOLOGY, Vol. 109, pp. 343–349.

McQueen, H. T., and Jonas, J. J., 1971, "Hot Workability Testing Techniques," *Metal Forming - Interrelation Between Theory and Practice*, Ed., A. L. Hoffmanner, Plenum Press, New York, pp. 393–428.

Roberts, W. L., 1983, *Hot Rolling of Steel*, Marcel Dekker, Inc., New York.

Sah, J. P., and Sellars, C. M., 1979, "Effect of Deformation History on Static Recrystallization and Restoration in Ferritic Stainless Steel," *Proc. Int. Conf. on Hot Working and Forming Processes*, Sheffield, England, pp. 62–66.

Sparling, L. G. M., 1977, "Load and Torque Determination for Hot, Flat Rolling with Variable Frictional Conditions," *Metals Technology*, Vol. 6, pp. 301–311.

Urcola, J. J., and Sellars, C. M., 1987a, "Effect of Changing Strain Rate on Stress-Strain Behaviour During High Temperature Deformation," *Acta Metall.*, Vol. 35, pp. 2637–2647.

Urcola, J. J., and Sellars, C. M., 1987b, "Influence of Changing Strain Rate on Microstructure During Hot Deformation," *Acta Metall.*, Vol. 35, pp. 2649–2657.

Urcola, J. J., and Sellars, C. M., 1987c, "A Model for a Mechanical Equation of State Under Continuously Changing Conditions of Hot Deformation," *Acta Metall.*, Vol. 35, pp. 2659–2669.

Wang, F., 1989, Ph.D. thesis, University of New Brunswick.

Watts, A. B., and Ford, H., 1952, "An Experimental Investigation of the Yielding of Strip Between Smooth Dies," *Proc. I. Mech. E.*, Vol. B1, pp. 448–453.

Weinstein, A. S., and Matsufuji, A., 1968, "Initial Report on Variable Strain Rate Effect on Deformation of Metals," *Iron and Steel Engineering*, Vol. 45, pp. 121–136.

Wray, P. J., 1986, "Modelling of Roll Force Behaviour in the Finishing Train of A Hot Strip Mill," *Proc. AIME Conf.*, Chicago, pp. 1–7.

Downloaded From: https://materialstechnology.asmedigitalcollection.asme.org on 06/29/2019 Terms of Use: http://www.asme.org/about-asme/terms-of-use